

Ph. Mertens, V. Thompson, G.F. Matthews, D. Nicolai, G. Pintsuk, V. Riccardo,
S. Devaux, B. Sieglin and JET EFDA contributors

Bulk Tungsten in the JET Divertor: Potential Influence of the Exhaustion of Ductility and Grain Growth on the Lifetime

“This document is intended for publication in the open literature. It is made available on the understanding that it may not be further circulated and extracts or references may not be published prior to publication of the original when applicable, or without the consent of the Publications Officer, EFDA, Culham Science Centre, Abingdon, Oxon, OX14 3DB, UK.”

“Enquiries about Copyright and reproduction should be addressed to the Publications Officer, EFDA, Culham Science Centre, Abingdon, Oxon, OX14 3DB, UK.”

The contents of this preprint and all other JET EFDA Preprints and Conference Papers are available to view online free at www.iop.org/Jet. This site has full search facilities and e-mail alert options. The diagrams contained within the PDFs on this site are hyperlinked from the year 1996 onwards.

Bulk Tungsten in the JET Divertor: Potential Influence of the Exhaustion of Ductility and Grain Growth on the Lifetime

Ph. Mertens¹, V. Thompson², G.F. Matthews², D. Nicolai¹, G. Pintsuk³, V. Riccardo²,
S. Devaux², B. Sieglin⁴ and JET EFDA contributors*

JET-EFDA, Culham Science Centre, OX14 3DB, Abingdon, UK

¹*Institute of Energy and Climate Research IEK-4 (Plasma Physics), Forschungszentrum Jülich,
Association EURATOM-FZJ, D-52425 Jülich, Germany, Member of the Trilateral Euregio Cluster*

²*EURATOM-CCFE Fusion Association, Culham Science Centre, OX14 3DB, Abingdon, OXON, UK*

³*Institute of Energy and Climate Research IEK-2 (Microstructure and Properties of Materials),
Forschungszentrum Jülich, Assoc. EURATOM-FZJ, D-52425 Jülich, Germany*

⁴*Max-Planck-Institut für Plasmaphysik, EURATOM Association, D-85748 Garching, Germany*

** See annex of F. Romanelli et al, "Overview of JET Results",
(23rd IAEA Fusion Energy Conference, Daejeon, Republic of Korea (2010)).*

Preprint of Paper to be submitted for publication in Proceedings of the
20th International Conference on Plasma Surface Interactions , Eurogress, Aachen, Germany
21st May 2012 - 25th May 2012

ABSTRACT

The divertor of the ITER-like Wall in JET currently includes a solid tungsten row for the outer strike point. The use of plasma-facing tungsten in fusion devices is limited by its brittleness in the low temperature domain and by the occurrence of grain growth at high temperatures. In the absence of active cooling, an extreme case of thermal cycling is represented by the situation in JET: the plasma-facing surface of the bulk tungsten tile experiences cyclic excursions from 200°C to about 2000°C. Thermal fatigue for impact factors of $11\text{--}24\text{MW/m}^2\sqrt{\text{s}}$ is investigated with a *Manson-Coffin* model; tungsten properties come from production samples. Recrystallization is studied in metallographic cuts of tungsten lamellae identical to those installed in the torus were exposed in the MARION facility to JET relevant heat fluxes for >300 pulses ($P_{dep} \leq 9\text{MW/m}^2$, angle of attack 6°). The calculations suggest that the number of high temperature cycles should be limited, especially if the grain growth degrades material properties.

1. INTRODUCTION

The divertor of the new JET ITER-like Wall (ILW) currently includes a solid tungsten row for the outer strike point. It is well known that the application of tungsten as plasma-facing material in fusion devices is limited by its brittleness in the low temperature domain [1] and by the occurrence of recrystallization at high temperatures [2,3]. Ideally, a narrow temperature window should be guaranteed for operation [4,5]. Extreme cases of thermal cycling at both ends of this range are represented by the JET tokamak on the one side and by the temperature range aimed at for DEMO on the other. With initial temperatures $\leq 200^\circ\text{C}$ and excursions of the temperature of the tile surface to a maximum of about 2000°C, the bulk tungsten material in JET undergoes –in the absence of active cooling– the worst possible cycling from this point of view, the driving reason for the complex design [6]. In contrast, tungsten would be kept in the planned DEMO “fingers” between 800°C and 1000°C [7,8]; that is well above the Ductile-to-Brittle Transition Temperature (DBTT) and below the domain of significant recrystallization. It would thus be much safer with respect to thermal cycling (we do not consider here neutron-induced damages).

The extreme conditions encountered in JET have motivated a closer look at the thermal fatigue of tungsten. The need for extreme care in this respect is underlined by experimental findings of recrystallization. As both effects cannot be avoided, they may well impose an upper limit to the total number of high performance pulses. The solid tungsten row in the divertor of JET consists of stacks of lamellae which are positioned as to mimic the former 3D shaped tile while retaining its shadowing properties in all directions (Fig.1). The basis for our study is thus either a single tungsten lamella or a full stack as shown in the figure.

2. THERMAL CYCLING AND FATIGUE

2.1 MATERIAL PROPERTIES

The analysis of thermo-mechanical fatigue relies on the knowledge of several material properties.

With the temperature range 200°C–2200°C subject of investigation, we have used either standard values for pure tungsten or, for some of them, those measured on pre-production samples collected during process qualification. The measured 0.2% yield and the ultimate tensile strength are shown in Fig.2 as an example. Note that the region of interest for fatigue lies where the temperature excursions are often well above the range where plentiful material data exist. Extrapolations had to be used in some cases to provide an adequate estimate for a full range temperature dependence of the material properties.

With a flux of 7–9 MW/m² for up to 10s, the thermal impact factors are in the range 11–24 MW/m² s. The study was initially carried out for a simplified, uniform heat input on the top, plasma-facing surface of a standard tungsten lamella (62×5.9×40 mm³) and later refined to a more representative wetted area of only 3.5 mm width in toroidal direction (the so-called “operational” case below). With consideration of the 1 mm gap between lamellae, the latter case corresponds to a local amplification of the heat flux of $6.9/3.5 = 1.97$.

2.2 RESULTS OF THERMAL CYCLING

The thermal and structural analyses were sequentially coupled in the course of seven cycles at different thermal impact factors, which is enough to reveal the main trend in the results. Several cases, corresponding to maximal temperatures of 1200°C, 1700°C and 2200°C were worked out. No allowance has been made for the additional effect of ELMs (edge localised modes) [9,10]. The non-linear thermal gradient through the lamella depth – from the plasma-facing surface down to the contact pads to the carrier – induce in the first place compression on the wetted front face and at the top of the racetrack channel which contains the clamping arrangement. Plasticity is taken into account by a material model which includes both kinematic and isotropic hardening to capture the behaviour as the stresses reverse direction during cycling [11].

A permanent deformation is visible in Fig. 3 which shows the level of plastic strain after the sixth pulse at the end of the cooling phase, i.e. back to 200°C. The figure applies to a uniform loading case. In comparison to the pure elastic calculation in ref. [12], the main stress in the upper part of the lamella (0–13 mm depth) has dropped from 150 MPa to about 120 MPa owing to the introduction of plasticity. Of course, incursion into the plastic domain is determined by the actual yield stress which is very much temperature dependent (Fig.2). As a consequence, the limiting yielding envelope for the poloidal stress and strain varies considerably with time. A small amount of strain ratchetting is observed, in the order of 5 µε per cycle. Whether this ratchetting rate eventually decreases with the number of cycles, thanks to the containment of the plastic zone within a purely elastic region, is unknown and out of the scope of the present analysis. The permanent deformations occur in the regions shown in Fig.3: the very top of the lamella (tagged 1), which is directly exposed to the high loads, and a small region at the upper extremities of the clamping hole (tagged 2). Note that this is a pure thermo-mechanical effect, independent of the clamping forces which correspond to a low, uniform pressure exerted on the bottom shoulder of lamella. These results are similarly valid for

the uniformly distributed loading and for the more realistic operational case in the sense that the same zones in the lamella are affected. The latter case presents an additional stress in the toroidal direction since the exposed region is partially constrained and the front face strain is peaked in toroidal direction due to the peaking in the heat flux and temperature. As a result, the total strain range on the plasma face reaches 600 to 2000 $\mu\epsilon$ as the temperature reaches values of 1200 to 2200°C. These values for the total strain range are used in the following section.

2.3 ESTIMATION OF THE FATIGUE LIFE

For the fatigue assessment of the mechanically driven stresses, we have selected a convenient form of the *Manson-Coffin* relation [13], the *Manson* equation from the method of “universal slopes” [14]. It compares favourably with experimental results for a wide range of materials and can possibly be put into place with the available tungsten data (also from Fig.2). Nevertheless, the fatigue predictions are based on an empirical correlation for general structure metals, including body-centred cubic crystalline structures, but are not specific to tungsten. The total strain range, elastic plus plastic, reads

$$\Delta\epsilon (N, \epsilon_f, \sigma_{UTS}, E) = \epsilon_f^{0.6} N^{-0.6} + 3.5 \frac{\sigma_{UTS}}{E} N^{-0.12}$$

where N is the number of cycles to failure, ϵ_f the true failure strain in tension, σ_{UTS} the ultimate tensile strength and E is Young’s modulus. Here the first term, which represents low cycle fatigue, dominates.

A representative picture of the expected fatigue life, according to this model, is shown in Fig. 4. The dashed curve (black squares) corresponds to a material which is close to room temperature whereas the blue one (diamonds) corresponds to 1200°C and the red colour (circles) to the highest temperature of 2200°C. The effect of temperature is only significant in the high cycle region because the elongation was assumed to be independent of temperature whereas E and σ_{UTS} are temperature dependent. The total strain range for the hottest case in section 2.2 amounted to 2000 $\mu\epsilon$ or $N=5000$ (arrows), without any margin.

Although the effect of the peak temperature is moderate—a factor of 1.5 to 2 at most between 1200°C and 2200°C—shorter pulse lengths, at fixed peak temperature, reduce the fatigue life: for the case “2200°C within 2 s,” the fatigue life without margin is less than 1000 cycles. Moreover, the degradation of tungsten properties above 1200°C due to recrystallization (grain growth) is not taken into account at this stage. It may obviously further reduce the fatigue life.

3. GRAIN GROWTH

Stacks of tungsten lamellae identical to those installed in the torus were exposed in the ion beam facility MARION [15,16] to JET relevant heat fluxes for more than 300 pulses ($P_{dep} \leq 9\text{MW/m}^2$, angle of attack 6°, $\sim 85\text{MW/m}^2$ on beam axis), roughly two thirds of which were

at temperatures above 1200°C. Details on the power deposition profile and results with respect to the overall power handling performance were reported elsewhere [17,18]. The exposed stacks contained a few prepared lamellae which were recrystallized, that is subjected to grain growth at different temperatures for 90 min. They are indicated in Fig.1:

- #10: a lamella in which grain growth has taken place during exposure only,
- #14: in oven at 1200°C prior to exposure,
- #16: in oven at 1400°C prior to exposure,
- #17: in oven at 1600°C prior to exposure.

All prepared lamellae were placed in the left portion of the prototype stack, which was exposed to the highest heat flux [17].

In the micrographs shown on Fig.5, all top faces, exposed to the plasma, are on the left side of the pictures. The various degrees of grain growth in different regions and in different lamellae are obvious:

- (a) the top picture shows the witness lamella, as delivered. It serves as witness to all others. The vertical orientation of the elongated grains ($\leq 32 \times 100 \text{ mm}^2$ according to ASTM E112: 2010), horizontal on the micrograph, was specified as the principal rolling direction;
- (b) lamella No.10 corresponds to the tokamak case. Grain growth has taken place in the upper part as indicated. It is mainly noticeable at the high loss in orientation (caution: with a scale of 200mm, the magnification is higher than in all other pictures);
- (c) c1-c3 correspond to lamellae 14 – 17, in order of increasing preparation temperature. The higher the temperature, the less visible is the frontier between the upper recrystallized zone and the lower structure which has remained as before exposure to the plasma.

Whether the grain growth provoked by the plasma bombardment results in a significant loss of mechanical properties is under investigation. We have first indications that the 0.2%– yield and the UTS can drop by as much as 40%.

In addition, a vertical section of lamella No.16 through the position indicated as – in Fig. 3 reveals the presence of a crack which extends perpendicularly to the clamping hole cut, in the direction of the front surface: Fig.6. It is about 3mm long. Remember that this lamella was recrystallized at 1400°C followed by an exposure to 100 low energy pulses and ~200 pulses at 40–65MJ/m², $\Delta t_{pulse} = 5 - 12\text{s}$. In the absence of statistics, this occurrence cannot be attributed unmistakably to the manufacturing process (electric discharge machining for that surface), to the cumulated effect of grain growth and thermo-mechanical fatigue, or even – which is less probable – to the sample preparation.

It may only draw our attention to the relative weakness of regions of high thermal stress, especially for metals with low fracture toughness when thermal fatigue plays a role in a zone of expected recrystallization.

CONCLUSIONS

When tungsten is used as plasma-facing material, especially in highly loaded zones, the possible occurrence of thermo-mechanical fatigue cannot be ignored. Estimates can be derived within the limits of a *Manson* model, which was deemed sensible if actual material data from production are fed in. Other boundary conditions to the thermal cycling, like detailed design, geometry of the loading, temperature extremes, characteristic times, etc. also play an important role. While cycling slightly into the plastic region and back, a certain amount of strain ratchetting comes to light. Precautionary measures, mainly budgeting of the high power pulses, were taken for JET to maximise the lifetime of the bulk tungsten tiles and somewhat relax the computed number of cycles to failure which amounted to 500 – 5000 depending on the chosen type of loading (highest vertical temperature gradient $\partial T/\partial z \leq 5 \times 10^4$ K/m, highest total strain range $\Delta \epsilon \leq 2000$ $\mu\epsilon$). The three temperature classes of (1001 – 1200°C), (1201 – 1700°C) and (1701 – 2200°C) may be used advantageously, in a pulse budget, to keep the possible damage within bounds. They provide the link to the realistic plasma scenarios which were proposed in [18].

Nevertheless, two worsening factors are not yet taken into account here above :

- the weakening of the material that is subject to high temperatures which results in appreciable grain growth. The evidence for an inevitable grain growth was shown experimentally with real components exposed to an ion beam in the MARION facility, under conditions made as close as possible to the exposure in the torus (peak power on axis $P \leq 85$ MW/m², incidence: angle of attack $\alpha \sim 6^\circ$). This may exacerbate thermal stress fatigue.
- the additional effect of ELMs which can significantly contribute to the material damage.

ACKNOWLEDGEMENTS

The authors are indebted to S. Brezinsek, Y. Krivchenkov and R. Neu who brought in their experience in numerous discussions. Their strong support is gratefully acknowledged. We also thank the MARION team and the JET team for swift operation of the respective facilities.

This work was supported by EURATOM and carried out within the framework of the European Fusion Development Agreement. The views and opinions expressed herein do not necessarily reflect those of the European Commission.

REFERENCES

- [1]. M. Rieth and A. Hoffman, *Fracture Behaviour of Tungsten based Alloys depending on Microstructure and Notch Fabrication Method*, Fusion Science and Technology **56** (2009) 1018-1022
- [2]. J. Linke, T. Loewenhoff, V. Massaut, G. Pintsuk, G. Ritz, M. Rödiger, A. Schmidt, C. Thomser, I. Uytendhouwen, V. Vasechko, M. Wirtz, *Performance of different tungsten grades under transient thermal loads*, Nuclear Fusion **51** (2011) 073017 (6pp)
- [3]. I. Uytendhouwen et al., *Mechanical properties and microstructural characterizations of*

- potassium doped tungsten*, Nuclear Engineering and Design **246** (2012) 198 – 202
- [4]. J. Schlosser, F. Escourbiac, M. Merola, S. Fouquet, P. Bayetti, J.J. Cordier, A. Grosman, M. Missirlian, R. Tivey and M. Rödig, *Technologies for ITER divertor vertical target plasma facing components*, Nuclear Fusion **45** (2005) 512 – 518
- [5]. A.R. Raffray et al., *High heat flux components—Readiness to proceed from near term fusion systems to power plants*, Fusion Engineering and Design **85** (2010) 93 – 108
- [6]. Ph. Mertens et al., *Clamping of solid tungsten components for the bulk W divertor row in JET—precautionary design for a brittle material*, Physica Scripta **T138** (2009) 014032 (5pp)
- [7]. P. Norajitra, R. Giniyatulin, V. Kuznetsov, I.V. Mazul, G. Ritz, *He-cooled divertor for DEMO: Status of development and HHF tests*, Fusion Engineering Design **85** (2010) 2251 – 2256
- [8]. P. Norajitra, S. Antusch, R. Giniyatulin, I. Mazul, G. Ritz, H.-J. Ritzhaupt-Kleissl, L. Spatafora, *Current state-of-the-art manufacturing technology for He-cooled divertor finger*, Journal of Nuclear Materials **417** (2011) 468 – 471
- [9]. K. Wittlich, T. Hirai, J. Compan, N. Klimov, J. Linke, A. Loarte, M. Merola, G. Pintsuk, V. Podkovyrov, L. Singheiser, A. Zhitlukhin, *Damage Structure in Divertor Armor Materials exposed to Multiple ITER relevant ELM Loads*, Fusion Engineering and Design **84** (2009) 1982 – 1986
- [10]. J. Linke, T. Loewenhoff, V. Massaut, G. Pintsuk, G. Ritz, M. Rödig, A. Schmidt, C. Thomser, I. Uytendhouwen, V. Vasechko, M. Wirtz, *Performance of different tungsten grades under transient thermal loads*, Nuclear Fusion **51** (2011) 073017 (6pp)
- [11]. Dassault Systèmes, SIMULIA-Abaqus, Technol. Brief TB-09-LCF-1 (2009)
- [12]. A. Borovkov, A. Gaev, A. Nemov, O. Neubauer, A. Panin, *3D finite element electromagnetic and stress analyses of the JET LB-SRP divertor element (tungsten lamella design)*, Fusion Engineering and Design. **82** (2007) 1871–1877, and V. Thompson, *Analysis of W-LBSRP End lamination for Chain Design*, JET Internal Report 1260/D004 (2008)
- [13]. G.E. Dieter, *Mechanical Metallurgy - SI Metric ed.* adapted by D. Bacon, McGraw-Hill Book Company (UK) Ltd, 1988 (751 pp.)
- [14]. S.S. Manson, *Fatigue: A Complex Subject - Some Simple Approximations*, The William M Murray Lecture 1964, Experimental Mechanics **5** (1965) 193-226
- [15]. M. Lochter, R. Uhlemann, J. Linke, Fusion Technology **19** (1991) 2101
- [16]. D. Nicolai, A. Charl, G. Czymek, M. Knaup, Ph. Mertens, O. Neubauer, A. Panin, H. Reimer, B. Schweer, R. Uhlemann, *Upgrade of the material ion beam test facility MARION for enhanced requirements of JET and ITER*, Fusion Engineering and Design **86** (2011) 2791–2794
- [17]. Ph. Mertens, H. Altmann, P. Chaumet, E. Joffrin, M. Knaup, G.F. Matthews, O. Neubauer, D. Nicolai, V. Riccardo, V. Tanchuk, V. Thompson, R. Uhlemann, U. Samm, *A bulk tungsten tile for JET: Heat flux tests in the MARION facility on the power-handling performance and validation of the thermal model*, Fusion Engineering and Design **86** (2011) 1801-1804

[18] Ph. Mertens, J.W. Coenen, T. Eich, A. Huber, S. Jachmich, D. Nicolai, V. Riccardo, K. Senik, U. Samm, and JET-EFDA contributors, Power handling of a segmented bulk W tile for JET under realistic plasma scenarios, *Journal of Nuclear Materials* **415** (2011) S943-S947

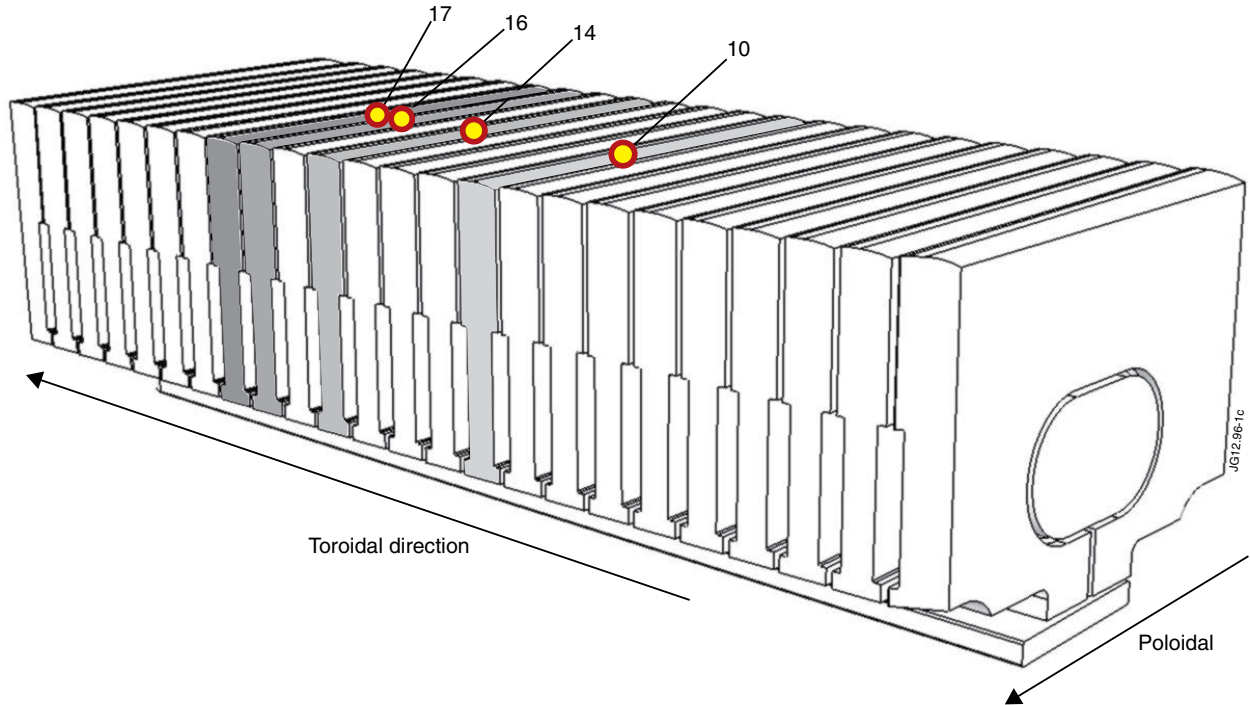


Figure 1: The main building block of the bulk tungsten tiles is a stack of 24 lamellae. The stacks are aligned with the toroidal direction. Shaded lamellae were undergoing recrystallization in an oven before exposure (Sect. 3)

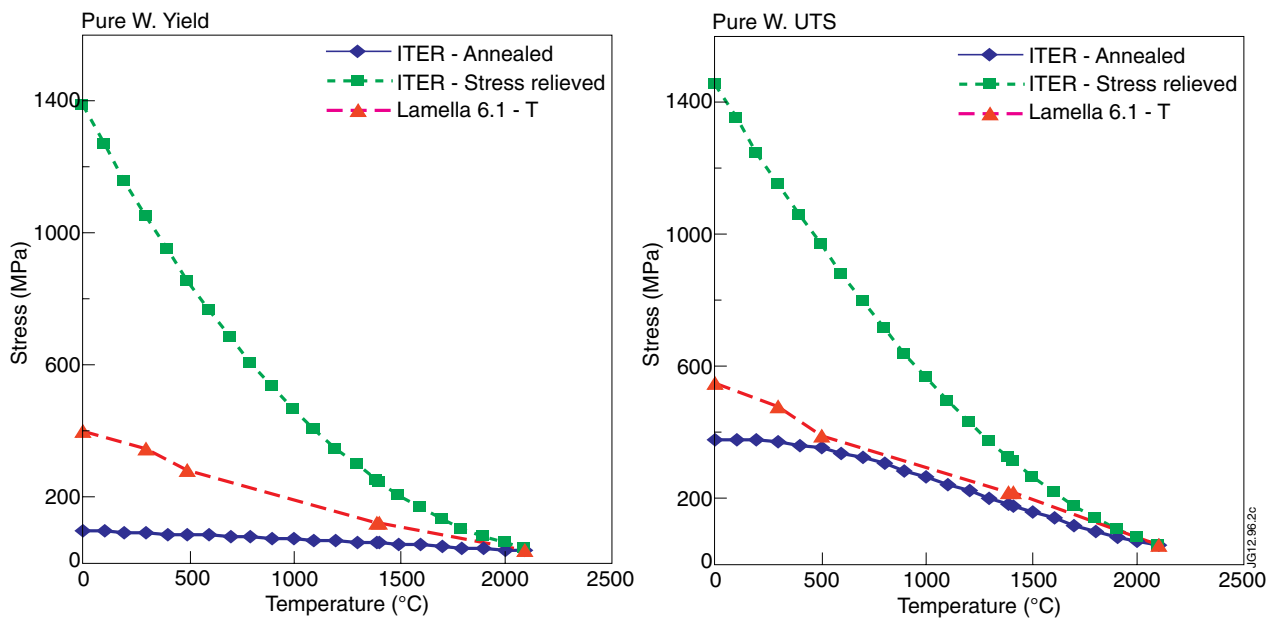


Figure 2: Tungsten yield (upper graph) and ultimate tensile strength (lower graph), both curves from actual samples. "T" indicates the somewhat weaker direction which is transverse to the main grain orientation as given by the last pass of the rolling process.

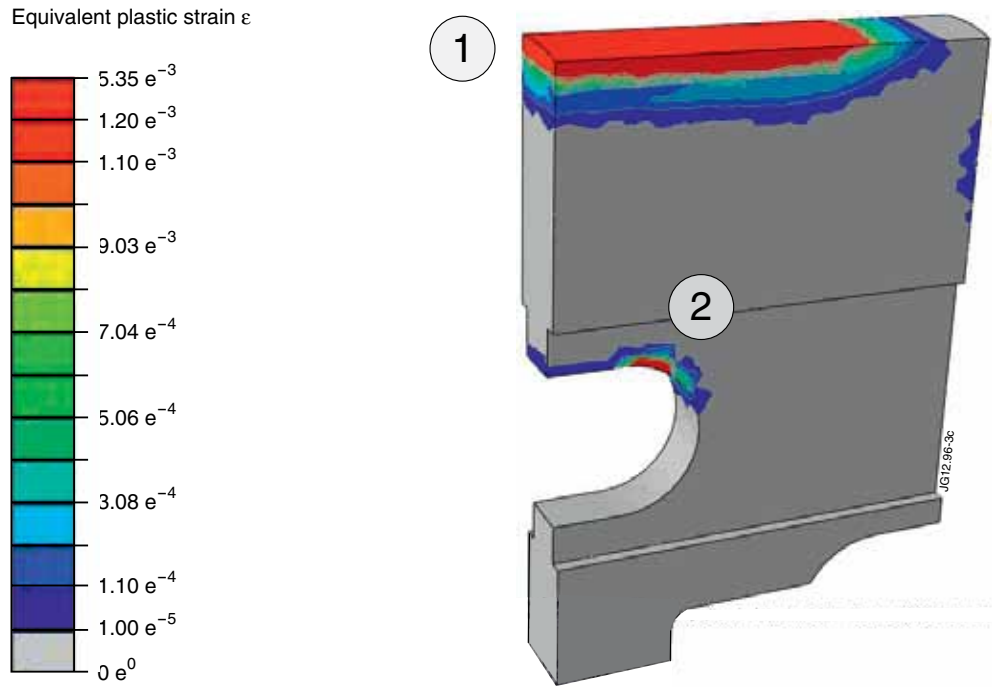


Figure 3: Plastic strain contours at the end of the 6th cycle at 9MW/m² for 10s (lamella cooled down back to the initial temperature). 1 and 2 mark the zones discussed in the text

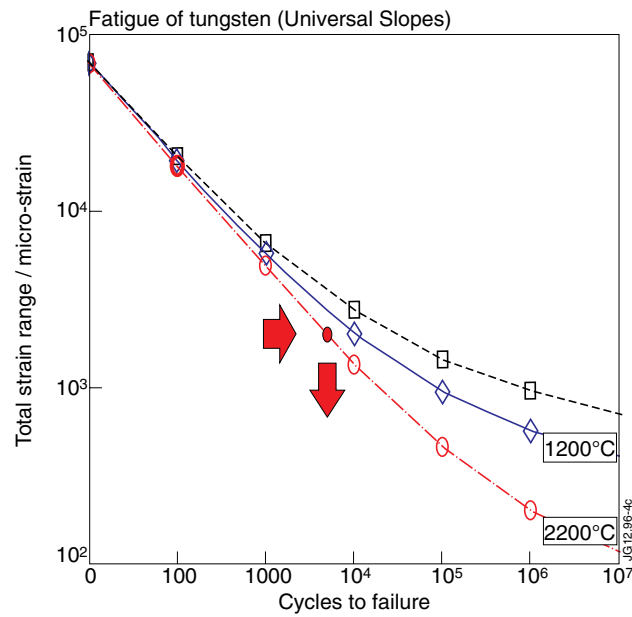


Figure 4: Fatigue of tungsten (method of the universal slopes). The arrows indicate the case discussed in section 2.2 with a computed total strain range of $2 \times 10^3 \mu\epsilon$

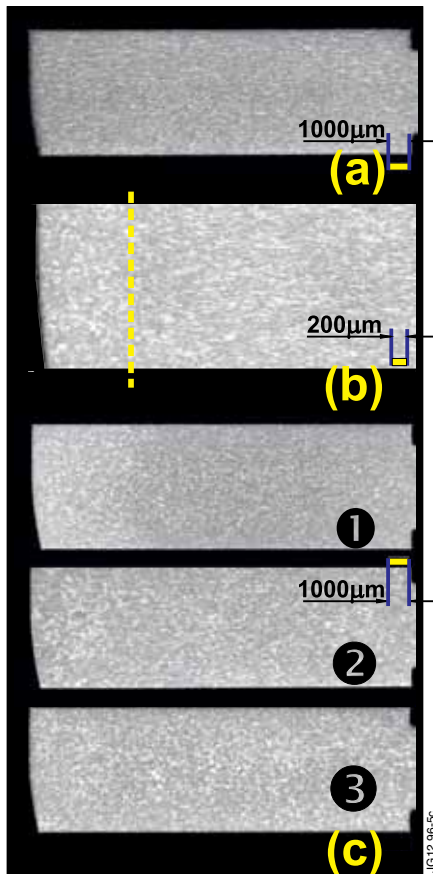


Figure 5: Micrographs: vertical cross-sections of different lamellae. The plasma-facing surface is on the left of the pictures. (a) unexposed witness lamella (scale 1 mm). The orientation of the elongated grains is clearly visible, it corresponds to the preferred rolling direction; (b) lamella no.10 (larger magnification: 200 μm): the border between recrystallized top and the lower part is indicated. Grains close to the front face are larger and have lost their orientation to a large extent. (c) various degrees of recrystallization before exposure: (1) 1200°C, (2) 1400°C, (3) 1600°C. After subsequent exposure: at higher grain growth temperatures in the oven, the frontier between recrystallization by the plasma and original material structure is barely visible.

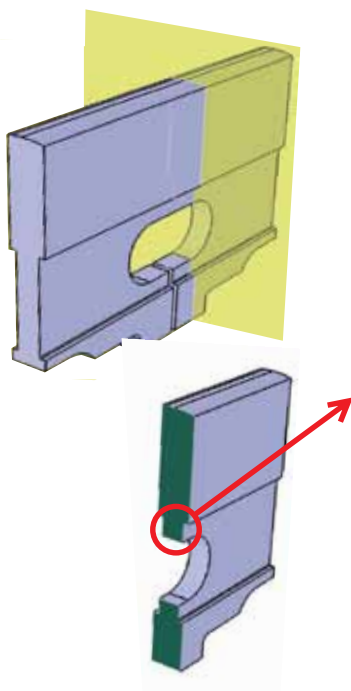


Figure 6: Crack found at the upper edge of the racetrack hole.